Smart Materials: Supramolecular Chiral Structures: Smart Polymer Organization Guided by 2D Polarization Light Patterns (Adv. Funct. Mater. 14/2012)

5 AUTHORS, INCLUDING:

Ulises Ruiz-Corona
Università della Calabria
29 PUBLICATIONS **211** CITATIONS

SEE PROFILE

Pasquale Pagliusi
Università della Calabria
81 PUBLICATIONS **700** CITATIONS

SEE PROFILE

C. Provenzano
Università della Calabria
44 PUBLICATIONS **298** CITATIONS

SEE PROFILE

Valery Petrovich Shibaev
Lomonosov Moscow State University
411 PUBLICATIONS **4,692** CITATIONS

SEE PROFILE

FULL PAPER

Supramolecular Chiral Structures: Smart Polymer Organization Guided by 2D Polarization Light Patterns

Ulises Ruiz, Pasquale Pagliusi, Clementina Provenzano, Valery P. Shibaev, and Gabriella Cipparrone*

Chiral periodic structures and photonic crystals have attracted a great deal of interest due to their applications in advanced photonics. As a consequence, the design and the fabrication of periodic microstructures in photosensitive materials have been widely investigated. Many achievements in the fabrication of such devices have been made over the last decade, but most of the established methods are still restricted to light intensity distribution with different structural shapes and minor attention has been devoted to exploit the vectorial nature of the light coupled with the response of polarization sensitive materials. Here, supramolecular chiral structuring in an amorphous azopolymer is demonstrated, coupling the strong and diversified photoresponse of the material with the holographic recording of 2D polarization patterns. The smart polymer organization guided by the complex light field induces periodic chiral microstructures, with spiral- or ribbon-like shape and identical or opposite helicity, characterized by high stability and complete reconfigurability. The holographic structures are theoretically described by means of the Jones matrix method and experimentally investigated, confirming the simultaneous presence of both linear and circular photoinduced anisotropies. These results prove an alternative approach to design a new class of materials with periodic chiral arrangement.

1. Introduction

In the last years the modern materials science has moved toward the study and the processing of smart functional materials exhibiting well-defined and complex functionalities. Artificial materials have been demonstrated which exhibit strong electric and magnetic responses aimed at manipulation of the amplitude, the direction, and the polarization of electromagnetic waves.[1–4] Recent studies addressed their attention also towards strategies to obtain reconfigurable materials able of performing an active control of their physical properties. Distinctive interest has been devoted to the investigations of gyrotropic media as potential candidates for achieving negative refraction and for applications in microwaves and opto-electronic devices, due to their ability of rotating the polarization state of the light by means of the chirality, both at the molecular and supramolecular levels. With this respect, artificial structures in metallic or dielectric media showing strong optical activity have been created adopting several approaches, as self-assembling and supramolecular chemistry, laser writing, lithographic techniques.[5–12]

Chirality shows interesting features even when organized in periodic 2D and 3D structures, because of their appealing applications in several areas of physics. Such structures, in fact, are potential candidates for photonic and opto-electronic applications, giving rise to strong optical activity,[13,14] circular dichroism,[15] or negative refraction.[16–19] Moreover, the design and the fabrication of 2D periodic microstructures and photonic crystals in photosensitive materials is a topic of considerable interest, for their applications in optical communication and sensing.[20–24] Holographic lithography-based techniques have emerged as a very promising approach for 2D structures and templates fabrications. They are generally based on the creation of 2D intensity distributions, obtained by managing the geometries of the interfering beams, namely the number of beams, the angles of incidence, the phase difference.[25,26] A space dependent refractive index modulation is generally induced in the photosensitive medium, which leads to the formation of different lattice structures. Beside the great interest addressed to intensity-based techniques, few efforts have been devoted to extend the approach exploiting the "vectorial nature" of light coupled with the diversified response of polarization sensitive materials.

Here we report on unique 2D reconfigurable periodic chiral structures recorded by means of vectorial holographic techniques in an amorphous azo-containing polymer film. This non-chiral polymeric material has revealed attractive features when irradiated with polarized light beam. Both linear and

Dr. U. Ruiz, Dr. C. Provenzano
Department of Physics
University of Calabria
Ponte P. Bucci, Cubo 33B, 87036, Rende CS, Italy
Dr. P. Pagliusi, Prof. G. Cipparrone
Department of Physics and CNR-IPCF
University of Calabria
Ponte P. Bucci, Cubo 33B, 87036, Rende CS, Italy
E-mail: gabriella.cipparrone@fis.unical.it
Prof. V. P. Shibaev
Chemistry Department
M. V. Lomonosov Moscow State University
Moscow, 119991, Russia

www.MaterialsViews.com

ADVANCED
FUNCTIONAL
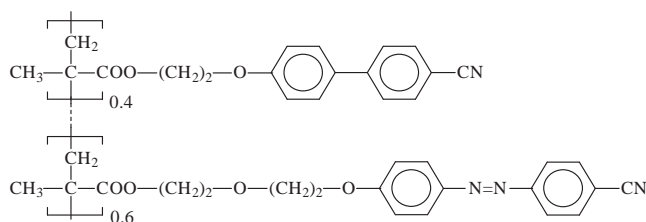MATERIALS
www.afm-journal.de

FULL PAPER

Figure 1. Chemical formula of the polymethacrylic copolymer.

circular birefringence occur when it is irradiated with linear and circular polarized light, owing to the light induced reorientation of the azobenzene molecular axis after multiple trans–cis–trans isomerization cycles.[27]

The specific characteristics of this material, related to high stability of the recorded structures and their complete reconfigurability, as well as its strong and diversified response to the light stimulus, make it a good candidate for the achievement of highly ordered periodic structures. We report on variously shaped periodic chiral lattices recorded on this polymer film. Taking advantage of the possibility to re-organize the material and exploiting the vectorial nature of the light, we have irradiated the polymer with complex light fields, having in mind the generation of 2D periodic chiral structures suitable for applications in holography, optical switching, addressing and other "smart" optical devices.

2. Material and Light-Assisted Structuring

The polymer used to perform the investigation is a side-chain copolymer with oxycyano-azobenzene fragments in the side chains whose chemical formula is reported in **Figure 1**.

The analysis of the material under polarized light[28] established that, beside the linear photo-induced birefringence, usual for azo-compounds, also a supramolecular chiral structure, whose handedness depends on the helicity of the light, is photo-induced in the polymer after irradiation with proper polarized light. Due to the different scale of the photo-induced processes, a different growth rate of the linear and circular birefringence versus the radiation dose is observed. For low intensity, the linear birefringence is about one order of magnitude higher than the circular birefringence. However, the latter rises much more prominently than the former, with the radiation dose, so that the difference between the two anisotropies is reduced. This means that a controlled irradiation enables to finely manage the photo-induced modifications and, as a consequence, the optical properties of the material. At last, the recorded structures exhibit a long-time stability at room

temperature, although they are completely erasable by thermal treatments above the glass transition temperature and optically reconfigurable.

The methodological approach to record the 2D periodic structures in the polymer film is based on a direct holographic writing, through a spatial light modulator (SLM)-assisted multi beams interference technique. According to the polarization states of the four writing beams, four light patterns have been implemented which belong to two extreme situations (see **Figure 2**). Indeed, the interference fields are either characterized by a uniform polarization state and a fully modulated intensity (Figure 2a,b), or by fully modulated polarization state and uniform intensity (Figure 2c,d).

In detail, the superposition of four plane waves with parallel linear (PLP) or circular (PCP) polarizations, produces the calculated polarization and intensity light patterns reported in Figure 2a,b, respectively. On the other hand, the interference of two pairs of plane waves with orthogonal linear (OLP) or circular (OCP) polarizations originates the polarization patterns sketched in Figure 2c,d, respectively. Here it is possible to see that the light intensity is almost uniform, while the spatial distribution of the polarization state is completely modulated from linear to circular polarization with various azimuthal angles and helicity values. Interesting spatial distributions of the polarization states are obtained, including linear, elliptical and circular polarizations that arrange in vortex periodic structures with opposite helicity. For all the four configurations, a phase shift of
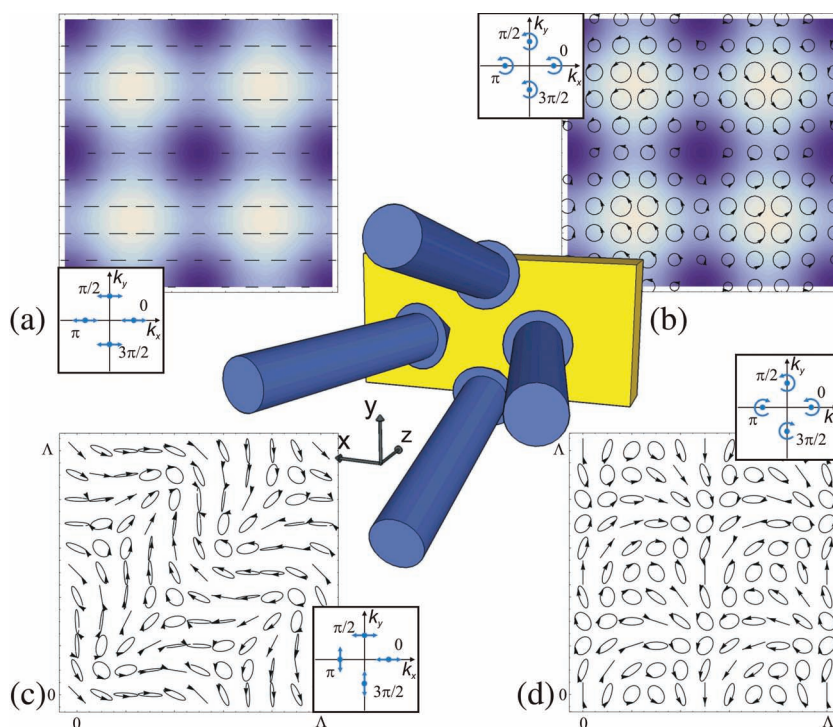

Figure 2. Schemes of the four–beam interference geometry (in the central part of the figure) and of the 2D light patterns generated by the four different configurations of polarization. Intensity and polarization patterns are reported for the PLP (a) and PCP (b) configurations. Pure polarization patterns occur for the OLP (c) and OCP (d) holographic configurations. Insets: schemes of the interfering waves in the k-space, showing their polarization and relative phases.
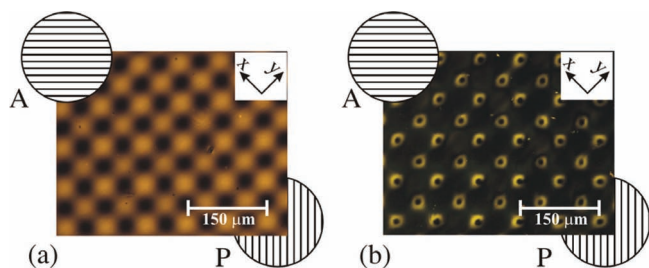
**ADVANCED
FUNCTIONAL
MATERIALS**

www.afm-journal.de

*Materials
Views*

www.MaterialsViews.com

FULL PAPER

Figure 3. Cross-polarized microscope images of the holograms recorded with the PLP (a) and PCP (b) configurations. The holograms are at 45° with respect to the polarizer (P) and the analyzer (A).

$\pi/2$ is introduced between each consecutive beam, as reported in the insets of Figure 2. In the case of intensity PLP and PCP configurations, the phase shift makes that the intensity distribution with parallel circular or parallel linear polarization in the interference region, arrange in a square lattice. In the case of OLP and OCP polarizations patterns, the phase shift contains the amplitude modulation of the optical field in the superposition region.

The polymeric film has been exposed to the interference fields generated by the four waves, at different irradiation doses. The resulting holograms, permanently stored in the polymer, have been investigated under the polarizing microscope and their far-field diffraction properties have been studied.

3. Results and Discussion

Figure 3a,b show the cross-polarized microscope images of the intensity holograms recorded by the interference fields reported in Figure 2a (i.e., PLP configuration) and b (i.e., PCP configuration). Both the PLP and the PCP holograms are oriented at 45° with respect to the crossed polarizers.

The PLP hologram in Figure 3a displays a square lattice structure of alternating bright and dark regions, which corresponds to the light intensity pattern of the interference field. Rotating the sample between the crossed polarizers, the bright regions became dark whenever the PLP hologram axes are parallel to the polarizers. This evidence supports the occurrence of a spatially modulated photo-induced linear birefringence in the polymer film, as expected for irradiation with linearly polarized light.

Similarly, the crossed-polarized image of the PCP hologram in Figure 3b exhibits a periodic square lattice characterized by bright circular structures. The latter shows a peculiar behavior when the hologram is rotated under the polarizing microscope, which resembles the one described in the reference[29] where an irradiation with a single circularly polarized Gaussian beam has been considered. The bright rings expand from or collapse towards their respective centers, depending on the rotation sense of the hologram (clockwise or anticlockwise) and on the helicity of the recording light. The annular-like geometry is related to the intensity profile of the interference light pattern, and its orientation-dependent variation can be accounted for by the light-guided formation of optical chiral supramolecular structures connected with the circular polarization.[29]
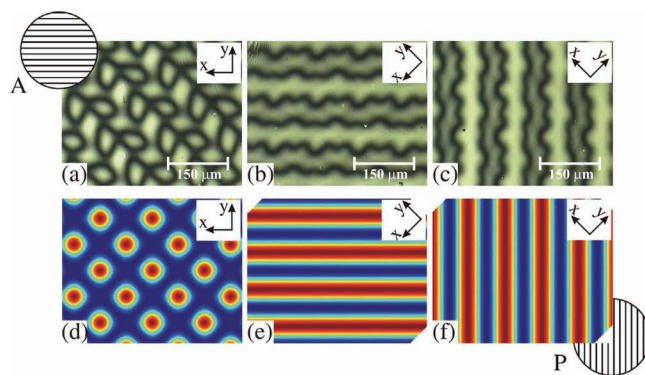

Figure 4. Cross-polarized microscope images of the holograms recorded with the OLP configuration for different orientations of the sample with respect to the polarizer (P) and the analyzer (A), namely 0° (a), −45° (b), and 45°(c). Simulations of the cross-polarized light intensity distribution for 0° (d), −45° (e), and 45°(f).
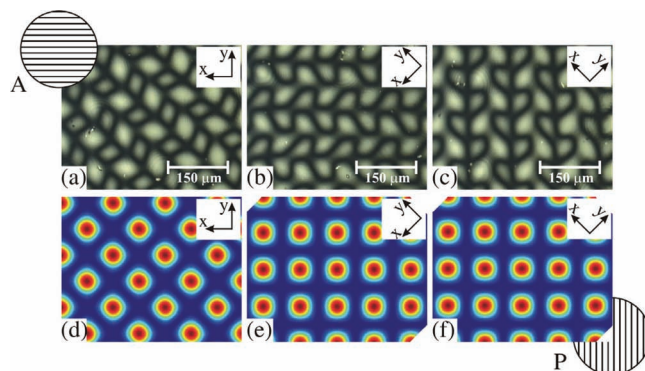

Figure 5. Cross-polarized microscope images of the holograms recorded with the OCP configuration for different orientations of the sample with respect to the polarizer (P) and the analyzer (A), namely 0° (a), −45° (b), and 45°(c). Simulations of the cross-polarized light intensity distribution for 0° (d), −45° (e), and 45°(f).

In **Figure 4** and **5** are reported the images of the structures recorded exploiting the light polarization patterns OLP and OCP shown in Figure 2c,d for low radiation dose.

In particular, Figure 4a–c shows the cross-polarized microscope images of the periodic structures recorded with the OLP configuration for different orientations of the sample with respect to the polarizers, namely 0°, −45° and 45°.

Similarly, Figure 5a–c reports the cross-polarized microscope images of the periodic structures recorded with the OCP configuration for the same orientations of the sample with respect to the polarizers. Although the Figure 4a and 5a look similar, the −45° and 45° images make evidence of a different optical behavior for the OLP and the OCP holograms, see Figure 4b,c and 5b,c. The cross-polarized images in Figure 4a–c and 5a–c have been simulated by means of the Jones formalism, in order to model the optical structures and, hence, infer the relative amplitude of the photo-induced linear and circular birefringence. Assuming a local photo-response of the medium, the Jones matrices of the OLP and OCP holograms are of the form

$$T_M^l = \exp\left(ikd\,\Delta n^l\right)\ (l = OLP,\,OCP) \tag{1}$$

www.MaterialsViews.com

ADVANCED
FUNCTIONAL
MATERIALS
www.afm-journal.de

FULL PAPER

in which k is the wave number, d is the thickness of the polymeric film and

$$\Delta n^l = \begin{bmatrix} \beta_s S_0 + \beta_{lin} S_1 & \beta_{lin} S_2 + i\beta_{cir} S_3 \\ \beta_{lin} S_2 - i\beta_{cir} S_3 & \beta_s S_0 - \beta_{lin} S_1 \end{bmatrix}^l. \quad (2)$$

The parameters β_s, β_{lin} and β_{cir} in Equation 2 are related to the photo-response, the photo-induced linear and circular birefringence of the material, respectively, while S_j are the Stokes parameters of the recording light field.[30] The latter are

$$S_0^{OLP} = 1$$
$$S_1^{OLP} = \sin\left[K(x - y)\right]$$
$$S_2^{OLP} = -[\cos(2Kx) + \cos(2Ky)]/2$$
$$S_3^{OLP} = -[\sin(2Kx) + \sin(2Ky)]/2 \quad (3)$$

and

$$S_0^{OCP} = 1$$
$$S_1^{OCP} = -[\cos(2Kx) + \cos(2Ky)]/2$$
$$S_2^{OCP} = [\sin(2Kx) + \sin(2Ky)]/2$$
$$S_3^{OCP} = \sin\left[K(y - x)\right] \quad (4)$$

for the OLP and OCP interference fields respectively, where $K = 2\pi/\Lambda$ and Λ is the spatial periodicity of the recorded structures.

The light field out of the hologram, oriented at an angle α between crossed polarizers, is

$$E_{out}^l = T_A R(-\alpha) T_M^l R(\alpha) T_P E_{in} \quad (l = OLP, OCP) \quad (5)$$

in which E_{in} is the microscope illumination field, R is the rotation matrix, T_P and T_A are the Jones matrices of the polarizer and the analyzer. The intensity light distribution of the OLP and OCP configurations, calculated from Equation 5, are

$$I^l = k^2 d^2 \frac{\sin^2 M^l}{(M^l)^2}\left[(\beta_{cir}^l S_3^l)^2 + (\beta_{lin}^l)^2\left(S_1^l \sin 2\alpha + S_2^l \cos 2\alpha\right)^2\right],$$

$$(6)$$

where $M^l = kd\sqrt{(\beta_{lin}^l)^2\left[(S_1^l)^2 + (S_2^l)^2\right] + (\beta_{cir}^l S_3^l)^2}$.

In Figure 4d–f and 5d–f we report the result of the simulations of the crossed-polarized images of the OLP and OCP holograms at 0°, –45° and 45°, by means of the Equation 6, for $\beta_{circ} \ll \beta_{lin}$. The different optical behaviours of the OLP and OCP holograms, recorded at low dosage, versus the angle α, are well simulated, suggesting that they can be accounted for by the sole photo-induced linear birefringence (associated with the polarization patterns). According to this finding, the brighter regions in Figure 4a and 5a correspond to the areas irradiated with linear polarization at 45°. They are expected to become dark when the holograms are rotated at –45° (Figures 4b and 5b) or 45° (Figures 4c and 5c), since the local optical axis turns out to be parallel to the polarizer or the analyser.

Nevertheless, some discrepancies exist between the images and the simulations, with the latter always showing higher symmetry in the shapes of the bright and dark areas with respect to the microscope images. Indeed, Figure 4a displays a slanted herringbone-like structure, while the simulation in Figure 4d
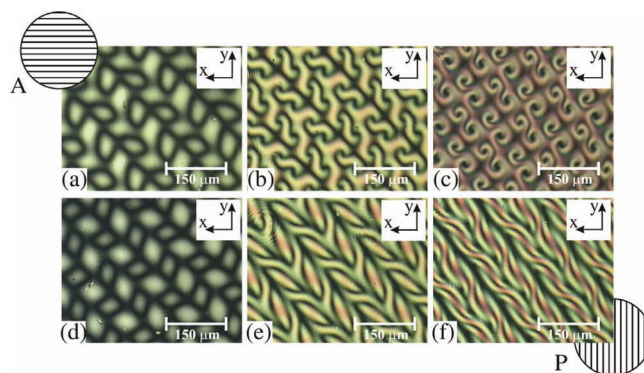

Figure 6. Cross-polarized microscope images of the OLP (a–c) and OCP (d–f) holograms recorded with increasing light dose: a,d) low (0.7 J/cm²), b,e) medium (7.0 J/cm²), and c,f) high (40.0 J/cm²) irradiation dosage. P-polarizer and A-analyzer.

exhibits a four-fold symmetry. Moreover, Figure 4b,c show that the horizontal and vertical bright lines are not straight as in the simulation. Analogously, the crossed-polarized images of the OCP holograms exhibit a herringbone-like structure, that rotates with the sample, instead of the four-fold structure shown by the simulation. These discrepancies are experimental artefacts, due to the imperfect orthogonality of the two planes of incidence of the recording beams.

Increasing the recording dose, the photo-induced circular birefringence becomes significant,[28] therefore the holograms evolve towards more complex structures, characterized by local chirality. In **Figure 6** we report the crossed-polarized microscope images of the OLP (Figure 6a–c) and OCP (Figure 6e–f) holograms for low, medium and high irradiation dose. A 2D array of spiral-like shaped structures, that alternate with opposite helicity, is achieved in the case of OLP configuration (Figure 6a–c). On the other hand, the OCP holograms develop towards 1D pattern of ribbon-like helices, with opposite handedness, characterized by enhanced anisotropy (Figure 6d–f).

The model of Equation 1, successfully adopted to simulate the optical behaviour of the OLP and OCP holograms recorded at low dosage, turns out to be inadequate to describe the corresponding optical structures obtained at higher dosage. Indeed, the model based on a local photo-response does not reproduce the experimental data, for any values of β_{lin} and β_{circ}. This result suggests that non-local effects, responsible for the supramolecular light-guided organization of the material,[29] should be considered to explain the microscope images in the case of high recording dosages.

To gain insight on the holograms recorded at medium irradiation dose, their far-field diffraction has been investigated in case of a linearly polarized probe beam. In **Figure 7** we report the pictures of the far-field diffraction patterns transmitted by the PLP (7a), PCP (7b), OLP (7c) and OCP (7d) holograms, when the probe beam is linearly polarized along the y-axis. From Figure 7a,b, it is evident that the diffraction patterns of the parallel polarized beams holograms exhibit a fourfold rotational symmetry (C_4), which is typical for a 2D intensity grating.[31,32] On the other hand, the diffraction patterns of the orthogonally polarized beams holograms in Figure 7 c,d show a
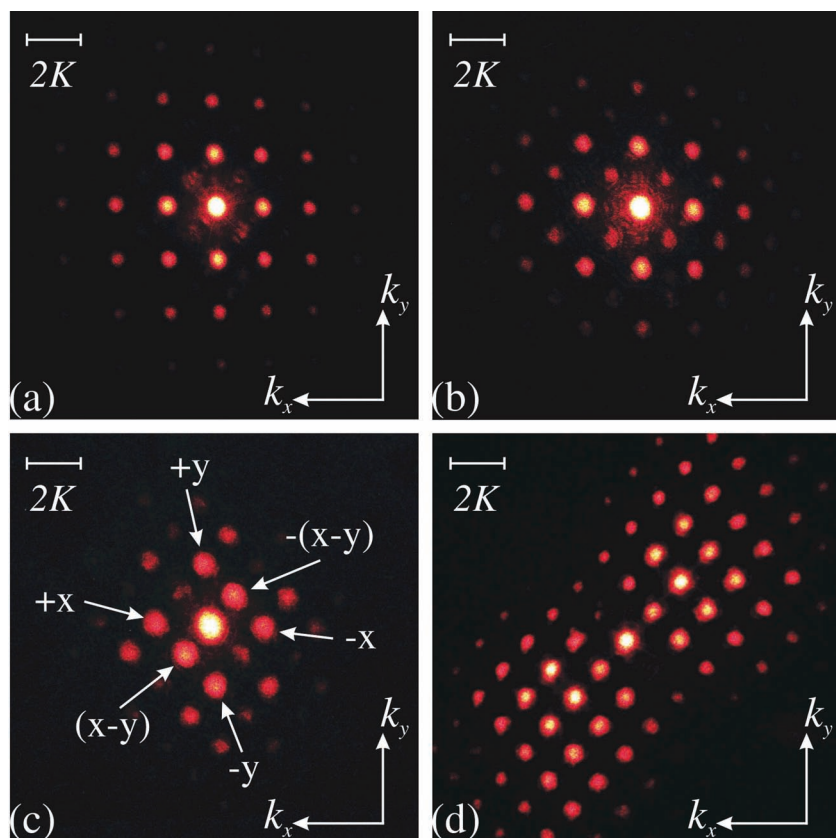
ADVANCED
FUNCTIONAL
MATERIALS
www.afm-journal.de

FULL PAPER

www.MaterialsViews.com

Figure 7. Far field diffraction patterns of a linearly y-polarized probe beam impinging on the PLP (a), PCP (b), OLP (c), and OCP (d) holograms.

twofold rotational symmetry (C_2), which are similar for the 2D polarization gratings.[33] In both cases, the symmetry degree of the diffraction patterns resembles the symmetry of the corresponding optical structures (see Figure 5 and 6).

The occurrence of both linear and circular birefringence in the orthogonally polarized configurations (OLP and OCP) has been verified by looking at the dependence of the intensity of the diffraction orders versus the polarization of the probe beam. In particular, in order to characterize the OLP configuration, the probe beam is passed through a quarter-wave plate and a polarizer before to hit the sample, and the intensities of the four diffraction orders (±x, ±y) have been measured versus the polarization direction α of the probe beam (see **Figure 8**a).

In Figure 8b we show that the efficiencies of the diffraction orders exhibit a biased harmonic dependence on the azimuth angle α, with the +x and +y orders having opposite phase with respect to the –x and –y orders. According to Equation 1 and assuming a linearly polarized probe beam $E_{in} = (\cos\alpha, \sin\alpha)$, the normalized intensities (i.e. the diffraction efficiencies) of the ±x and ±y diffraction orders are given by

$$\eta_{\pm x,\pm y} \equiv \frac{I_{\pm x,\pm y}}{I_{in}} \cong \frac{d^2 k^2}{16}\left[\beta_{lin}^2 + \beta_{circ}^2 \mp 2\beta_{lin}\beta_{circ}\cos(2\alpha)\right], \quad (7)$$

adopting the Jones formalism.[28] The assumption of the local photo-response of the medium is satisfactory for the holograms recorded at intermediate irradiation dose. The diffraction

efficiencies in Equation 6 exhibit a harmonic dependence on the azimuthal angle α, which reproduces the observed behaviour, provided that both β_{lin} and β_{circ} are non-zero. In particular, $\beta_{lin} = 4.7 \times 10^{-3}$ and $\beta_{circ} = 1.5 \times 10^{-3}$ have been evaluated by fitting the experimental data reported in Figure 8b.

Looking at the diffraction pattern produced by the OCP grating, we can find a further confirmation of the presence of both the linear and circular photo-induced birefringences. In this case, in fact, Figure 7d shows that the first ±x and ±y orders of diffraction (i.e., $\vec{k}_{\pm x} = \pm 2K\hat{x}$ and $\vec{k}_{\pm y} = \pm 2K\hat{y}$, respectively) are present as well as the first ±(x–y) orders (i.e. $\vec{k}_{\pm(x-y)} = \pm K(\hat{x} - \hat{y})$). Differently from the previous case (i.e. the OLP grating), the diffraction efficiency of all the orders is independent from the azimuthal angle α, which is proportional to β_{lin} (i.e. $\eta_{\pm x,\pm y} \cong d^2 k^2 \beta_{lin}^2/8$) for the first ±x and ±y diffraction orders, and to β_{circ} (i.e. $\eta_{\pm(x-y)} \cong d^2 k^2 \beta_{circ}^2/4$) for the first ±(x–y) orders.

4. Conclusions

Supramolecular chiral periodic structuring of an amorphous azo-polymer is demonstrated, exploiting the sensitivity of the material to the light, in the completeness of its vectorial nature. Selected 2D light patterns, coupled with the local and non-local material response to the optical field, permit the formation of spiral- and ribbon-like chiral structures. A four-beams holographic approach has been adopted in order to manage the intensity and the polarization of the writing light field in a bidimensional periodic fashion. An optical characterization of the structured polymer film is reported, which is based on the cross-polarized microscope imaging and the far-field diffraction analysis. The analysis suggests that the local photo-induced linear birefringence is responsible of the material structuring at low irradiation dose, and that a non-local response, in which both linear and circular birefringence are induced by the light stimulus, predominates at high dosage, when the suprastructural chiral patterning occurs. Taking advantage of the unique characteristic of the polymer and of its response to the light stimuli, we demonstrate the possibility of building, in a very simple way, optical architectures of great complexity. The results suggest an alternative way to design new class of supramolecular chiral materials, characterized by high stability and complete reconfigurability, which have potential advantages for applications in smart functional devices.

5. Experimental Section

Materials: The polymer used to perform the investigation is a side-chain polymethacrylic copolymer with 60 mol% content of oxycyano-azobenzene fragments in the side chains of the
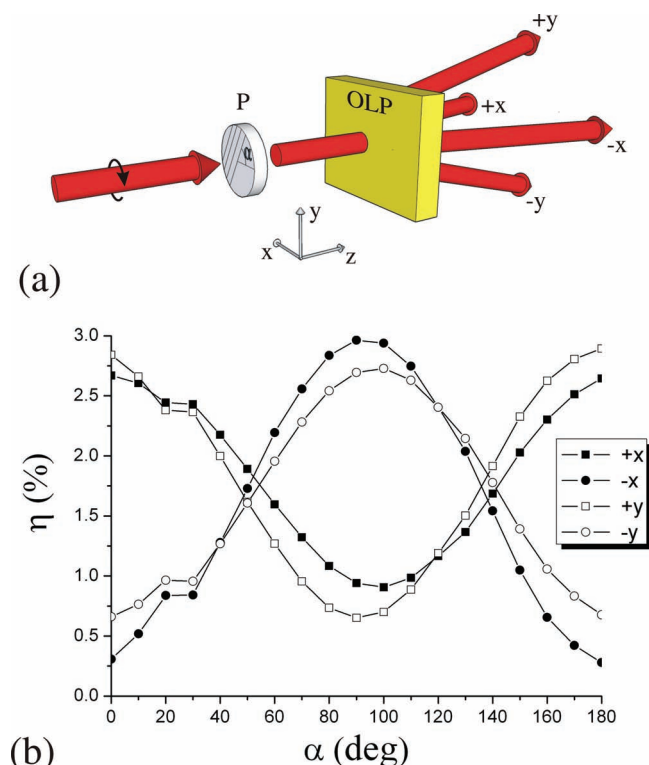
Figure 8. a) Experimental set-up for measuring the polarization dependent diffraction intensities of the OLP hologram. The circularly polarized probe beam is passed through a polarizer (P) in order to vary the angle α of the polarization plane. b) The intensity of the $\pm x$ and $\pm y$ diffraction orders is reported versus the polarization direction α of the probe beam.

macromolecule. The synthesis of the copolymer (polymerization degree Pn = 43; polydispersity = 2.44) is described in References.[34,35] The glass transition temperature of the polymer is $T_g = 77$ °C. The sample is a 10 μm thick film confined between two glass plates, prepared by melting the polymer above the T_g and cooling it down to room temperature. The confining substrates avoid the formation of surface reliefs in the experiments.

Experimental Setup: an Argon laser beam of wavelength $\lambda = 488$ nm impinges on a phase-only spatial light modulator (SLM, PLUTO, Holoeye Photonics AG), which, through a synthetic phase hologram, generates four plane waves linearly polarized along the x-axis. The interference of these latter creates the PLP light pattern, while the PCP configuration is achieved by passing the four beams through a quarter-wave plate. The OLP configuration is obtained rotating the linear polarization of a pair of consecutive beams of 90° with respect to the other two by means of a half wave plate, whereas for the OCP geometry the four plane waves pass through a quarter-wave plate placed after the half wave plate. The light patterns generated by the interfering waves have a spatial periodicity $\Lambda = \lambda/\sin\theta \approx 150$ μm, which depends on the angle of incidence of the beams θ, that in the adopted geometry is the same for all the interfering fields, and on the wavelength of the light λ. A more detailed description of the recording set up is reported in Reference.[36]

Methods: Three different light irradiation regimes have been employed in the holographic recording experiments: low, 0.7 J/cm², medium 7 J/cm² and high dosage 40 J/cm².

A linearly probe beam, polarized along the y-axis, from a He-Ne laser whose wavelength ($\lambda = 633$ nm) is far from the absorption band of the polymer, has been used to investigate the diffraction properties of the holograms recorded at medium irradiation dose, in the PLC, PCP, OLC and OCP configurations.

[1] T. J. Yen, W. J. Padilla, N. Fang, D. C. Vier, D. R. Smith, J. B. Pendry, D. N. Basov, X. Zhang, *Science* **2004**, *303*, 1494.

[2] J. Y. Ou, E. Plum, L. Jiang, N. I. Zheludev, *Nano Lett.* **2011**, *11*, 2142.

[3] M. Lapine, I. V. Shadrivov, D. A. Powell, Y. S. Kivshar, *Nat. Mater.* **2012**, *11*, 30.

[4] M. A. C. Stuart, W. T. S. Huck, J. Genzer, M. Müller, C. Ober, M. Stamm, G. B. Sukhorukov, I. Szleifer, V. V. Tsukruk, M. Urban, F. Winnik, S. Zauscher, I. Luzinov, S. Minko, *Nat. Mater.* **2010**, *9*, 101.

[5] S. Shang, *Nat. Biotechnol.* **2003**, *21*, 1171.

[6] A. Hirst, B. Escuder, J. Miravet, D. Smith, *Angew. Chem. Int. Ed.* **2008**, *47*, 8002.

[7] S. K. Y. Tang, R. Derda, A. D. Mazzeo, G. M. Whitesides, *Adv. Mater.* **2011**, *23*, 2413.

[8] M. S. Rill, C. Plet, M. Thiel, I. Staude, G. von Freymann, S. Linden, M. Wegener, *Nat. Mater.* **2008**, *7*, 543.

[9] M. Deubel, G. von Freymann, M. Wegener, S. Pereira, K. Busch, C. M. Soukoulis, *Nat. Mater.* **2004**, *3*, 444.

[10] E. R. Dedman, D. N. Sharp, A. J. Turberfield, C. F. Blanford, R. G. Denning, *Photonics Nanostruct.* **2005**, *3*, 79.

[11] S. Lee, H. S. Kang, J. K. Park, *Adv. Funct. Mater.* **2011**, *21*, 1770.

[12] S. Lee, J. Shin, H. S. Kang, Y. H. Lee, J. K. Park, *Adv. Mater.* **2011**, *23*, 3244.

[13] M. Decker, M. Ruther, C. E. Kriegler, J. Zhou, C. M. Soukoulis, S. Linden, M. Wegener, *Opt. Lett.* **2009**, *34*, 2501.

[14] E. Plum, V. A. Fedotov, A. S. Schwanecke, N. I. Zheludev, *Appl. Phys. Lett.* **2007**, *90*, 223113.

[15] M. Decker, M. W. Klein, M. Wegener, S. Linden, *Opt. Lett.* **2007**, *32*, 856.

[16] R. Shelby, D. R. Smith, S. Schultz, *Science* **2001**, *292*, 77.

[17] B. Li, G. Sui, W. H. Zhong, *Adv. Mater.* **2009**, *21*, 4176.

[18] E. Plum, J. Zhou, J. Dong, V. A. Fedotov, T. Koschny, C. M. Soukoulis, N. I. Zheludev, *Phys. Rev. B* **2009**, *79*, 035407.

[19] N. I. Zheludev, *Science* **2010**, *328*, 582.

[20] L. Vogelaar, W. Nijdam, H. van Wolferen, R. M. de Ridder, F. B. Segerink, E. Fluck, L. Kuipers, N. F. van Hulst, *Adv. Mater.* **2001**, *13*, 1551.

[21] J. W. Kang, M. J. Kim, J. P. Kim, S. J. Yoo, J. S. Lee, D. Y. Kim, J. J. Kim, *Appl. Phys. Lett.* **2003**, *82*, 3823.

[22] J. H. Holtz, S. A. Asher, *Nature* **1997**, *389*, 829.

[23] Y. J. Lee, P. V. Braun, *Adv. Mater.* **2003**, *15*, 563.

[24] J. Huang, X. B. Hu, W. X. Zhang, Y. H. Zhang, G. T. Li, *Colloid Polym. Sci.* **2008**, *286*, 113.

[25] Y. M. C. Timothy, T. Ovidiu, J. Sajeev, *Phys. Rev. E* **2006**, *71*, 046605.

[26] Y. J. Hung, S. L. Lee, Y. T. Pan, B. J. Thibeault, L. A. Coldren, *J. Vac. Sci. Technol. B* **2010**, *28*, 1030.

[27] S. Xie, A. Natansohn, P. Rochon, *Chem. Mater.* **1993**, *5*, 403.

[28] G. Cipparrone, P. Pagliusi, C. Provenzano, V. P. Shibaev, *J. Phys. Chem. B* **2010**, *114*, 8900.

[29] G. Cipparrone, P. Pagliusi, C. Provenzano, V. P. Shibaev, *Macromolecules*, **2008**, *41*, 5992.

[30] L. Nikolova, P. S. Ramanujam, *Polarization Holography*, Cambridge University, Cambridge **2009**.

FULL PAPER

[31] D. Xu, K. P. Chen, K. Ohlinger, Y. Lin, *Appl. Phys. Lett.* **2008**, *93*, 031101.

[32] J. Xavier, P. Rose, B. Terhalle, J. Joseph, C. Denz, *Opt. Lett.* **2009**, *34*, 2625.

[33] C. Provenzano, P. Pagliusi, G. Cipparrone, *Opt. Express* **2007**, *15*, 5872.

[34] S. Belayev, T. Zvetkova, Y. Panarin, S. Kostromin, V. Shibaev, *Vysoko-molek. Soedin., Seris B* **1986**, *28*, 789.

[35] A. N. Simonov, D. V. Uraev, S. G. Kostromin, V. P. Shibaev, A. I. Stakhanov, *Laser Phys.* **2002**, *12*, 1294.

[36] U. Ruiz, C. Provenzano, P. Pagliusi, G. Cipparrone, *Opt. Lett.* **2012**, *37*, 311.